

Silicon Anodes for Lithium-Ion Batteries Based on a New Polyimide Binder

David Lusztig,^[a] Shalom Luski,^[a] Netanel Shpigel,^[b] Naresh Vangapally,^[a] and Doron Aurbach^{*[a]}

Silicon is a promising candidate for replacing graphite in anodes for advanced Li-ion batteries due to its high theoretical gravimetric energy density. However, silicon as an active anode material suffers from significant volume changes upon lithiation/delithiation, causing fast capacity fading. The performance

of silicon anodes depends on the polymeric binders used, which form well-bound Si particles matrices that accommodate the strains developed during their repeated lithiation, thus maintaining their integrity.

Herein, we investigated the effect of thermal treatment on the performance of polyimide P84 as a novel binder for composite Si anodes comprising metallurgical micron-size silicon particles (80% silicon). The electrochemical behavior of metallurgical silicon-based anodes heat-treated to 120 °C, 200 °C, 300 °C, and 400 °C was examined in half (vs. Li electrodes) and full (vs. NCM622 cathodes) cells. An optimal performance was obtained after heat treatment at 400 °C, related to the very good adhesion of the electrode's active mass to the current collector, and the ability of the heat-treated binder to enhance the active mass integrity upon cycling.

A comparison between optimized anodes developed herein to jnl Si anodes containing frequently used binders like Sodium Alginate (SA) and Lithium Polyacrylate (LiPAA), demonstrated clear advantages of the heat-treated Si anodes containing P84. This study opens the door for the use of very cost-effective Si anodes comprising relatively cheap binders and easily processable commercial metallurgical micrometric size Si particles.

The demand for materials with higher specific capacity leads to silicon-based anode materials. Typically, lithium-ion cells contain graphite-based anodes with a specific capacity of about 370 mAh/g (fully lithiated graphite, i.e., LiC₆ compound). Silicon is particularly promising, potentially reaching a specific capacity near 3750 mAh/g when forming Li_{4.4}Si, roughly ten times higher than graphite. It is abundant, low-cost, and has a favorable working voltage of about 0.3–0.4 V with respect to Li/Li⁺.^[5–9]

Nonetheless, despite years of research and development, silicon-rich anodes with high capacity have not yet been commercialized. Si anode-based Li-ion batteries seem not mature yet, although this may be imminent. Silicon is a semiconductor and suffers from massive volume changes (volume changes up to 300%) during the lithiation (alloying) process. This phenomenon causes diverse negative effects on any silicon electrode, including - pulverization, high internal stress, delamination, and defective passivation because protective and stable surface films cannot be developed and remain stable on a surface area that changes periodically.^[10]

Commercial Li-ion batteries, like those from Tesla and Panasonic, contain silicon in their anodes, albeit as a minor component alongside graphite. However, some companies claim to produce complex, mature, high-capacity silicon-based anode materials. For instance, Sila Nano's and Group 14 utilize carbon-coated nanoporous silicon, while Amprius manufactures silicon nanowires through a unique CVD method, and Enovix designed three-dimensional cells, reducing the volume significantly compared to traditional cells.^[11–14] So, it is clear that the high specific capacity of Li–Si anodes drives impressive innovative efforts to develop effective Si anodes for advanced Li batteries.^[11–17]

However, innovative materials that include nano-particles may not be cost-effective. Consequently, despite the above efforts, Li-ion batteries based on Si anodes cannot be considered a commercial reality. This situation encourages further efforts to develop Si anodes based on low-cost raw materials, and it can be mitigated by controlling the structure of the composite silicon electrodes.^[7,18,19] Many efforts have been invested in the past 20 years to alleviate the problems of Si electrodes using various strategies. One of them was using

Introduction

Lithium-Ion batteries (LIBs) are the most attractive electrochemical power sources due to their high energy density. Yet, future energy consumption and power demands are predicted to increase. Electric vehicles needing longer driving distances and the demand for longer operation periods of mobile devices require batteries with higher gravimetric and volumetric energy density.^[1–4]

[a] Mr. D. Lusztig, Dr. S. Luski, Dr. N. Vangapally, Prof. D. Aurbach
Department of Chemistry, Institute of Nanotechnology and Advanced Materials (BINA), Bar-Ilan University
and

INIES – Israel National Institute of Energy Storage, Ramat-Gan 5290002, Israel
E-mail: doron.aurbach@biu.ac.il

[b] Dr. N. Shpigel
Department of Chemical Sciences, Ariel University, Kiryat Hamada 3, Ariel 40700, Israel

compatible and improved binders. Binders adhere the active material particles and the conductive agent to the current collector. They are often used in small amounts but yet may be crucial in preserving the electrochemical performance of composite electrodes comprising highly reactive materials.^[10,20]

PVDF (polyvinylidene difluoride) is the most important binder in electrodes for Li-ion batteries, including graphite anodes. However, it is incompatible with silicon high-capacity anodes due to its low volume variations capabilities, and it binds with active electrodes' materials mainly in weak Van Der Waals bonds, which are insufficient to sustain the vast volume changes and consequent cracking of composite Si electrodes.^[18,21,22]

Over the years, numerous binder alternatives to PVDF, such as CMC, Li/Na-Alginate, PAA, and LiPAA, have been investigated. These binders improved the performance of composite Si electrodes, but what was achieved was insufficient for use in proper industrial batteries. Nonetheless, although binders alone cannot prevent the self-destructive processes of silicon electrodes, well-designed binders can alleviate the side effects of cracking and significantly improve their performance.^[7,19,23–25]

Due to their unique chemical and physical properties, polyimides have recently been identified as potential anode binders for lithium-ion batteries. As a class of high-performance polymers, polyimides exhibit excellent thermal stability, chemical resistance, mechanical strength, and enhanced adhesion, making them promising candidates for improving the performance and safety of rich silicon lithium-ion batteries.^[26–28]

One common use of polyimides is as a dielectric material in electronic devices, where it is used to insulate copper electrical contacts with jnl components. Copper-to-polyimide bonding is frequently accomplished through a thermal curing process. It involves heating the polyimide to initiate a chemical reaction that forms covalent bonds to the copper surface. The exact curing process may vary depending on the specific polyimide and copper materials used, the desired bonding strength, and jnl properties.^[26,28–32] We used a co-polymerized polyimide binder denoted as P84 (3,3,4,4-benzophenone-tetracarboxylic dianhydride (BTDA)), with 80% toluene diisocyanate (TDI) and 20% methylene diphenyl diisocyanate (MDI), and according to the manufacturer's datasheet (Evonik), P84 molecular weight is higher than 125,000 g/mol.^[33] It is heat stable, adheres to copper, and is soluble in ordinary solvents. Compared to PVDF, P84 can accommodate silicon volume changes and has higher adhesion strength. Choi, J. et al. (2015) demonstrated that substituting PVDF with P84 as a binder improves silicon anodes' cycle life in lithium-ion batteries.^[23,24,34,35] Thermal heating of P84 can also affect its intrinsic properties and enhance the performance of silicon anodes. When the polyimide is heated above 300 °C, its tensile strength, elongation, Young's modulus, and molecular weight increase.^[36–38]

Therefore, we aimed to examine the influence of thermal treatments of P84 as a binder for silicon anodes based on low-cost metallurgical micrometric silicon particles. We used various heat treatments temperatures, 120 °C, 200 °C, 300 °C and 400 °C. These selected temperatures are below and above T_g (around 315 °C–320 °C) and all below the thermal decomposition

temperature, T_d=525 °C.^[36,39] We believe that developing practical high-capacity anodes for Li-ion batteries based on this metallurgical silicon is an important goal because it can increase their energy density and yet reduce cost.

Experimental

To investigate and compare the effect of the thermal treatment of silicon electrodes with P84 binder on cells' performances, composite electrodes containing micrometric size metallurgical silicon and P84 as a binder were heated to various temperatures – 120 °C–400 °C. The electrodes were assembled into half (Vs. Lithium) and full (Vs. NCM 622, BASF, Germany) pouch cells. The cells were examined by galvanostatic charge-discharge cycling and post-mortem analyses by HR-SEM and XPS.

Silicon electrodes were composed of 80% metallurgical micrometric size silicon (Average particle size 1.5 μm, Ferroglobe PLC, Spain), 10% P84 (Ensinger, Germany) as a binder, and the conductive additives were 7.8% Graphene (XGSciences, USA), and 2.2% MWCNT (Arkema, France). All components were first mixed and stirred in the solvent N-Methyl-2-pyrrolidone (NMP, Biolab, Israel).

Then, the mixtures were mixed in a Thinky, planetary centrifugal vacuum mixer up to 3 times at 2000 RPM for 3 minutes each. Next, this slurry was coated on copper foils (Optek Ltd, China), a one-sided layer using the "Doctor blade" technique at a typical loading of 3 mg/cm² and then dried overnight at 120 °C under vacuum and then calendered in a rolling mill (IRM, USA). The coated foils then were cut to the desired proposed dimensions of 35 mm×30 mm for pouch cells.

The dried electrodes were heated in a tube furnace (Carbolite Gero, United Kingdom) to temperatures of 120 °C (i.e., no extra heating), 200 °C, 300 °C, and 400 °C in an inert nitrogen atmosphere. The heating rate was 10 degrees per minute, the dwell time was 1 hour, and the system naturally cooled to room temperature.

Pouch cells containing heat-treated silicon electrodes, Li metal counter electrodes for half cells, and commercial NCM 622 electrodes (BASF, Germany) as cathodes for full cells in a typical loading of 30 mg/cm² were assembled under pure argon atmosphere in a glove box. Porous polyethylene separators (Celgard 2500, USA) were used, and the electrolyte solutions were added to all cells (1 M LiPF₆ DMC:FEC 4:1 by Gotion, Inc. USA), and then the pouch cells were sealed. The cells were stored overnight at room temperature to ensure proper electrodes wetting by the electrolyte solution.

The cells were tested at a constant temperature (30 °C) by galvanostatic charge-discharge cycling method using an LBT21084 battery cycler (Arbin Instruments, USA).

All cells experienced the same formation process, which consisted of running the cells for three cycles at a low current rate (C/10) up to a limited charging capacity (1500 mAh/g of silicon) to stabilize the cells, particularly the passivation of the Si electrodes by their surface films, while the de-lithiation voltages were 1.0 V (maximum) in half cells and lithiation voltage of 2.75 V (minimum) in full cells. After formation cycles, the cells were degassed and then were run at a working current rate (C/3) during 50 cycles for half cells and 300 cycles for full cells in a working voltage of 0.1 V–1.0 V and 2.75 V–4.1 V for half and full cells respectively. After completing their runs, the cells underwent post-mortem analysis. The electrodes were examined and characterized compared to pristine electrodes, which were taken before the cells were assembled. Morphol-

ogy images were produced using high-resolution scanning electron microscopy (HR-SEM- Magellan XHR 400L FE-SEM, FEI, USA).

Results and Discussion

Electrodes were heat treated and assembled into cells. The cells were cycled and analyzed to investigate the effect of the heat treatment that the Si anodes containing P84 binder underwent on the cells' performance. The only difference between all the electrodes containing the P84 binder was their heat treatment temperatures. Yet significant differences were observed.

Galvanostatic Cycling

Half Cells (Vs. Li Metal)-Comparison of P84-Based Anodes after Heat Treatments at Various Temperatures

Figure 1a shows results from periodic cycling experiments of half cells (Si vs. Li), demonstrating that after 50 cycles, the cells

containing 400 °C heat-treated Si anodes remained at anodes specific capacity of approximately 1100 mAh/g, while the specific capacity of anodes in cells with 300 °C and 200 °C heat-treated Si anodes dropped to 500 mAh/g and 20 mAh/g, respectively, and the cells with untreated electrodes lost their entire capacity during short cycling periods. The coulombic efficiencies of the cells containing anodes that were cured at 400 °C were stable at approximately 99.6% after the fifth cycle.

The same trend was observed in the formation cycles, as demonstrated by the voltage profiles presented in Figure 1b. The electrochemical response of cells containing untreated Si electrodes (i.e., electrodes that were cured up to 120 °C only) exhibited fast degradation and decreasing coulombic efficiency. In turn, the cells containing Si electrodes, heat-treated up to 400 °C, demonstrated stabilization within their first three cycles, during which their specific capacity increased to around 1470 mAh/g.

The derivatized voltage responses – dq/dV vs. V curves also exhibit the same trend. Figure 2a shows curves related to the 5th, 20th, and 40th cycles of cells with untreated Si anodes (i.e., cured at 120 °C) and cells with heat-treated Si anodes at 400 °C.

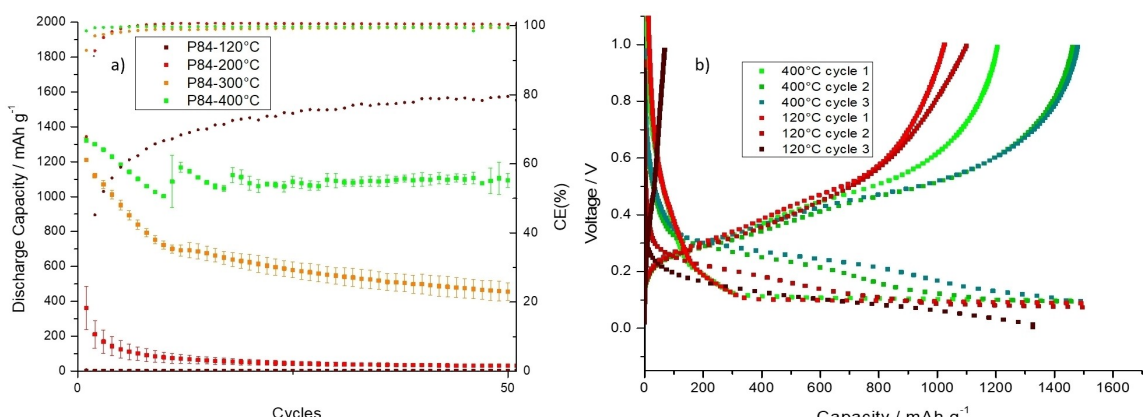


Figure 1. Composite silicon electrodes containing P84 binder, cycled galvanostatically in half cells (vs. lithium) containing 1 M LiPF₆ solutions in DMC-FEC 4:1. a) Average discharge capacities and coulombic efficiencies as a function of cycle number operated at 0.1–1.0 V, electrodes heat-treated to 120 °C, 200 °C, 300 °C, and 400 °C are compared (as marked therein). b) Voltage profiles of 3 formation cycles operated up to 1.0 V (vs. Li) limited by capacity up to 1500 mAh/g, electrodes heat-treated to 120 °C and 400 °C are compared (as marked therein).

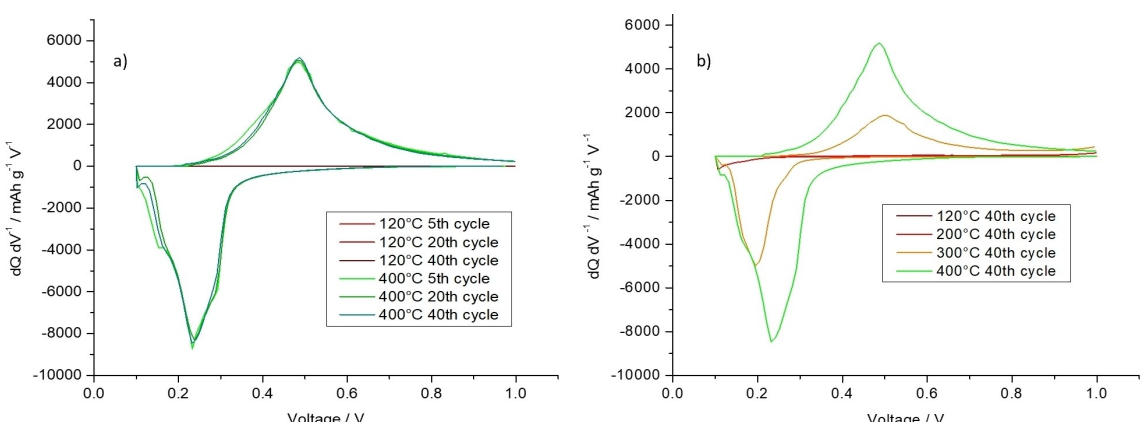


Figure 2. dq/dV vs. V curves of composite silicon electrodes containing P84 binder in half cells (vs. Li CE) with 1 M LiPF₆ solutions in DMC:FEC 4:1 in the potential range 0.1–1.0 V of a) heat-treated to 120 °C and 400 °C (as indicated) in 5th, 20th, and 40th cycles, and b) 40th cycle of Si–|Li comparing composite Si/P84 electrodes heat-treated to 120 °C, 200 °C, 300 °C, and 400 °C, as indicated.

Figure 2b shows similar curves related to the 40th cycle of cells with Si electrodes heat-treated at 120 °C, 200 °C, 300 °C, and 400 °C.

The curves in Figure 2a demonstrate the stable behavior of the composite Si electrodes treated at 400 °C (a stable set of two corresponding redox peaks), and the negligible capacity (no peaks) of the untreated electrodes. Both charge and discharge peaks of heat-treated electrodes at 400 °C remain relatively constant and do not change much over the cycling experiments, with the main lithiation process occurring between 0.23–0.24 V, which is typical and likely for a-Si->a-Li_xSi_y phases, probably Si->Li₂Si process. The de-lithiation peak around 0.45 V corresponds to the reversed process, Li₂Si->Si.^[40–42]

A similar pattern can be observed in Figure 2b, where the response is most pronounced for the electrodes treated at 400 °C and is lower as the treatment temperatures drop. Hence, the same phenomenon is observed in all the temperatures. The peaks in Figure 2b reflect the redox behavior of Li–Si electrodes being charged to 1500 mAh/g in the initial lithiation process, which probably forms Li₂Si.^[4,42]

Full Cells – (Si Anodes vs. NCM 62 Cathodes)

To further demonstrate the heat treatment effect on the Si anodes containing the P84 binder (heated to the range 120 °C–400 °C), pouch cells containing the Si anodes and cathodes comprising commercial LiNi_{0.6}Co_{0.2}Mn_{0.2}O₂ (NCM 622) were prepared and tested.

The same trend was observed with full cells as for half cells (Figure 3a and Figure 3c). After 300 cycles, the full cells with anodes heat-treated to 120 °C faded severely. The Si anodes heat-treated to 200 °C reached after 300 cycles to a specific capacity of around 60 mAh/g. With the anodes heat-treated at 300 °C, the final specific capacity reached in these experiments was around 250 mAh/g. In turn, full cells with composite Si anodes heat-treated to 400 °C reached after 300 cycles in full cells to the highest final specific capacity, around 560 mAh/g, nearly 1/3 of their initial specific capacity, as presented in Figure 3a. It should be emphasized that this result is far from being satisfactory. Loosing nearly 66% of specific capacity in cycling experiments of about 300 cycles is totally unacceptable for anodes in rechargeable Li-ion battery prototypes.

However, although the results presented here are far from the elementary practical requirements, clear trends are seen: Using the lower cost form of silicon and relatively easily prepared composite electrodes, we demonstrate a path for

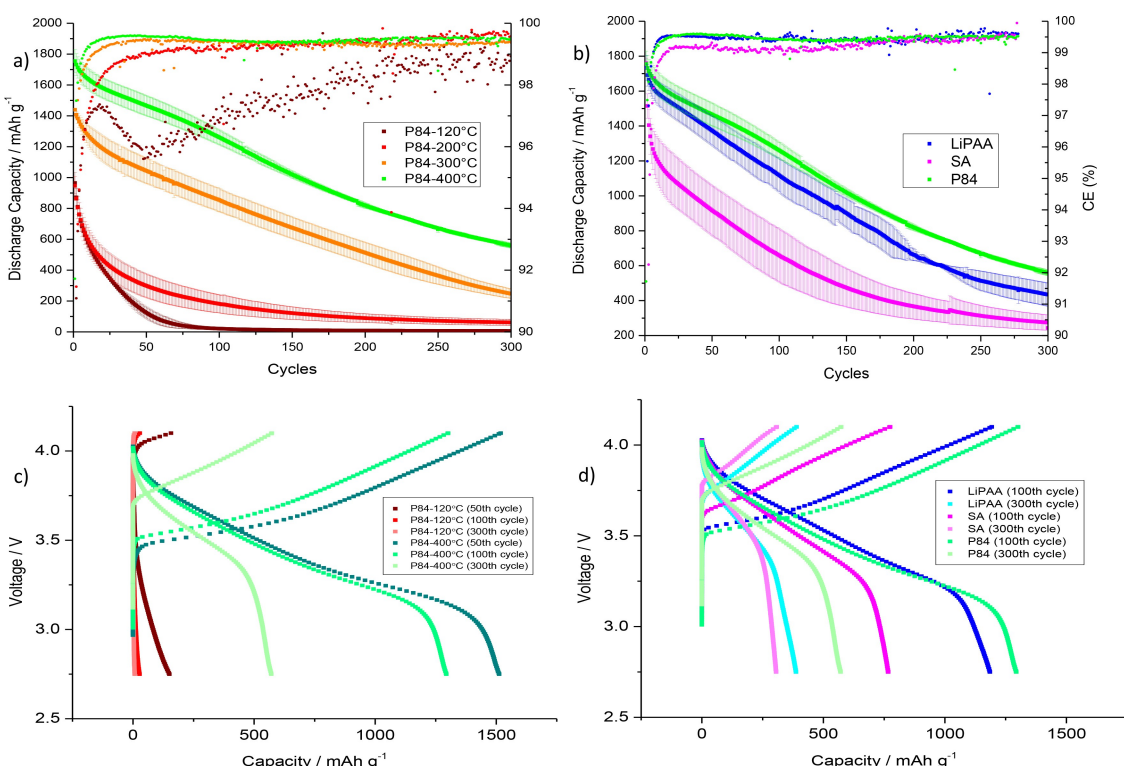


Figure 3. a) Discharge capacities and coulombic efficiency of silicon/P84 anodes cycled galvanostatically in full cells vs. NCM622 cathodes as a function of cycle number during 300 cycles. 1 M LiPF₆ DMC:FEC 4:1 solutions. Cells with composite anodes heat-treated to 120 °C, 200 °C, 300 °C, and 400 °C (as indicated) are compared. b) Average discharge capacities and coulombic efficiency as a function of cycle number of full cells: silicon/P84 (400 °C) anodes vs. NCM622 cathodes and 1 M LiPF₆ DMC:FEC 4:1 solutions, compared to similar cells in similar experiments which composite Si anodes were based on sodium alginate and LiPAA binders. c) Voltage profile of silicon/P84 anodes cycled galvanostatically in full cells vs. NCM622 cathodes at the 50th, 100th, and 300th cycle operated between 2.75 V–4.1 V (vs. NCM). Cells with composite anodes heat-treated to 120 °C and 400 °C (as indicated) are compared. d)–Voltage profile of full cells: silicon/P84 (400 °C) anodes vs. NCM622 cathodes at the 100th and 300th cycle operated between 2.75 V–4.1 V (vs. NCM), compared to similar cells in similar experiments in which composite Si anodes were based on sodium alginate and LiPAA binders.

optimization by heat treatment of composite electrodes containing polymeric matrices that change properties via relatively simple thermal processes. These leave a playground for further optimization for stabilizing high specific capacity, relatively simple, and cheap silicon anodes for advanced Li-ion batteries.

Comparison with Na Alginate and LiPAA Binders

The favorite Si anodes containing P84 binder heat-treated at 400 °C were compared in full cells cycling experiments to similar Si anodes containing sodium alginate (SA) and lithium polyacrylate (LiPAA) binders, which are considered advanced binders for Si anodes compared to the commonly used PVDF binder. The results are presented in Figure 3b and Figure 3d. Indeed, the heat-treated P84 containing Si anodes performed far better than the electrodes containing the sodium alginate and LiPAA binders. After 300 cycles, the average capacities retained (after a starting specific capacity of around 1800 mAh/g) were 550, 450, and 300 mAh/g for Si anodes containing P84, LiPAA, and SA binders, respectively (Figure 3b and Figure 3d). The trend

was also clear at the 100th cycle. The specific capacity of P84 was the highest in comparison to LiPAA and SA. These results further emphasize the potential of the heat-treated P84 binder to revolutionize the performance of composite high-capacity Li–Si anodes.

Post-Mortem Analysis of Cycled Electrodes, Visual Tests

After cycling, the anodes were separated from the cells and were washed with dimethyl carbonate (DMC). As presented in Figure 4a, the active mass of untreated electrodes (i.e., heating up to 120 °C) could be easily peeled off from the current collector after cycling. With all jnl electrodes, the composite active mass (containing the heat-treated P84 binder) remained adhered well to the current collectors, but the electrodes heat-treated to 200 °C appeared to have the best adhesion between the current collector and the composite active mass, whereas with the electrodes heat-treated to only 200 °C, the active mass of the cycled electrodes examined, began to peel away from the sides.

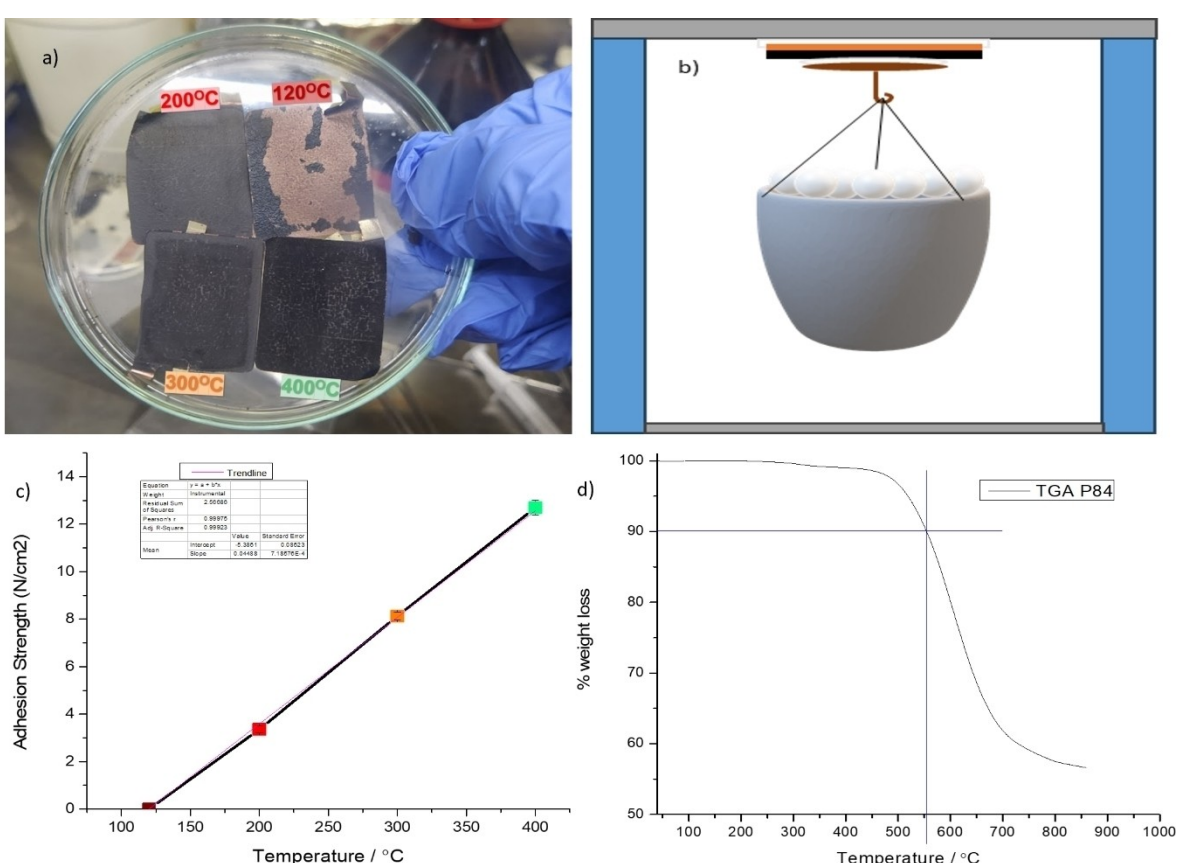


Figure 4. a) Post-mortem analysis of composite silicon anodes containing P84, cycled in half-cells vs. Li counter electrodes with 1 M LiPF₆ solutions in DMC:FEC 4:1, tested for mechanical stability after 50 working cycles. The heat treatment temperatures of the electrodes are marked. b) Schematic drawing of the in-house tester. From top to bottom: A Plastic (grey), double-sided adhesive (white), the copper side of the electrode, the active mass side of the electrode (black), double-sided adhesive (white), hook (brown), cup (grey), and marbles (white). c) Results of pulling-off tests for the cycled composite Si electrodes heat-treated before cycling at different temperatures. The force required to pull off the P84 containing composite active mass from the Cu foils current collectors is plotted as a function of the electrodes' curing temperature. The conditions of cycling: Galvanostatic cycling at C/3 rate, 50 cycles, vs. Li counter electrodes, and the electrolyte solution was 1 M LiPF₆ DMC:FEC 4:1. d) Thermogravimetric analysis (TGA) results of P84 powder in an inert atmosphere.

Pulling-Off Tests

Pulling-off tests were assessed to examine how well the active mass of the electrodes was adhered to the Cu foils current collectors. An in-house prepared tester was used to carry out these measurements. The electrodes were cut, and two 3 M 300LSE double-sided adhesive tapes were applied to both sides of the tested electrodes. The copper current collector side was adhered onto a clean plastic at the instrument's top head, while the anode active material side was attached to a round metal hanger (diameter of 12 mm) and connected to a cup. Twenty-five grams of marble particles were added to the cup one by one, gradually increasing the gravitational force until the active materials detached (a schematic drawing of the tester is represented in Figure 4b).

The adhesion test results of all the pristine electrodes we prepared and tested before undergoing any electrochemical exceeded our maximal measuring capabilities, meaning that the active material adhered more strongly to the current collector than the adhesive tape, demonstrating excellent initial adhesion of the active mass to the current collectors even when the heat treatment reached no more than 120 °C.

Due to the volume change phenomenon of Si anodes during cycling, the results for the post-cycled electrodes were different. The heating temperature of the anodes strongly affected the adhesion in a linear trend: the higher the electrode's curing temperature - the higher the force required to separate the composite cycled active mass from the Cu foil current collector, as presented in Figure 4c. The electrodes became more robust and could not be dismantled in these tests as the heat treatment temperature was higher. The electrodes cured at 120 °C were easily peeled off and could not hold any force. The cycled electrodes heat-treated at 200 °C, 300 °C, and 400 °C could be separated (composite active mass from the current collector) when the applied force reached values of 3.34, 8.11, and 12.70 N/cm², respectively, displaying significant differences between the samples, and the fitting results showed a very good linear adjusted R-square exceeded 0.999.

These pull-off test results comply with the electrochemical tests results. There is a clear correlation between good adhesion, which is a function of the electrodes' curing temperature, and good cycling stability of the electrodes.

The thermal stability of the polyimide binder was characterized using thermogravimetric analysis (TGA) in an inert atmosphere. As per the literature, P84 is resistant and can withstand temperatures exceeding 400 °C, whereas its massive decomposition commences at temperatures exceeding 500 °C. According to its manufacturer (Evonik), 10% Weight loss in the air occurs at 525 °C, while 10% weight loss in nitrogen occurs at 570 °C.^[33]

Our test results are consistent with the literature. A minor weight loss was observed, primarily as a result of impurities and cross-linking reactions at temperatures below 500 °C, which can be regarded as the decomposition onset temperature. Only at approximately 550 °C did the material experience a 10% weight loss, indicating mass decomposition.

Analysis of Cycled Electrodes by HR-SEM and EDX Measurements

HR-SEM analysis was performed on pre-cycled pristine electrodes and post-cycled electrodes heat-treated to 120 °C, 200 °C, 300 °C, and 400 °C.

No significant changes were observed within the samples taken before cycling in all magnifications (Figure 5).

After 50 cycles, dramatic changes were observed.

In the samples of heat-treated electrodes to 120 °C, the silicon particles were covered by a thick layer of decomposition products. This observation became less visible as the heat treatment temperature of the electrodes was higher.

In post-mortem analyses of cycled electrodes heat-treated to 400 °C, the silicon particles could be observed, indicating the remaining integrity of these electrodes. In addition, as a result of the silicon volume changes during cycling, all electrodes' samples exhibit by SEM imaging more cracks than the samples of electrodes before cycling (Figure 6). These morphological changes are explained by part of the capacity degradation seen with all of these electrodes after 300 cycles.

This post mortem analysis by SEM shows that when the composite electrodes explored herein were cured at lower temperatures than 400 °C, the heat-treated binder could not sufficiently adhere the silicon particles together and to the current collector. As a result, the periodic volume change of the silicon particles upon cycling badly affects their integrity, passivation, and stability. When the integrity of the composite structure is poor (if the binder is not effective enough), there are more detrimental side reactions with the electrolyte solution during cycling, preventing the stabilization of the electrodes' passivation by robust SEI type surface layers. A morphological instability enables the electrolyte solution to percolate through the active mass, reaching the current collector and reacting on it (between the composite active mass and the Cu foil current collector). This situation is detrimental to a good adherence between the active mass and the current collector. The heat treatment at high enough temperatures forms covalent bonds within the P84 and good enough interactions between the cured binder and the copper that strengthen the adhesion (mainly above T_g).

The silicon volume changes processes during lithium and de-lithium alloying imply considerable stress, tension, and stretching forces on the copper, as evidenced by its rugged surface following cycling. Before cycling, the adhesion of all electrodes was satisfactory, but after cycling, detrimental performances and delamination were examined in the 120 °C electrodes compared to higher heat-treated electrodes. This suggests that the issue most likely does not lie in the active material adherence to the copper.

The SEM images also correlate with the coulombic efficiency of both half and full cells. From the first cycle, the 120 °C heat-treated silicon electrodes exhibit the lowest ICE, improving as the heat-treated temperatures increase to 400 °C. The failure starts during the first cycles, affecting the cells' performances and shortening their life afterward.

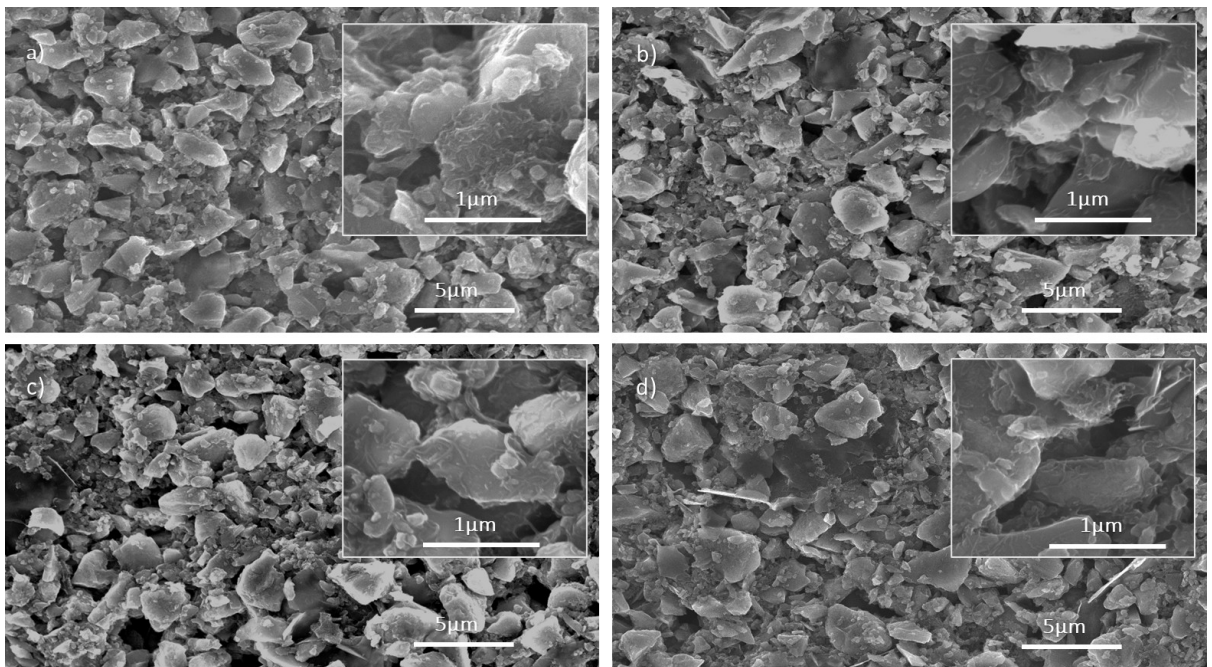


Figure 5. HRSEM images of pre-cycled composite silicon electrodes containing P84 binder heat-treated to a) 120 °C, b) 200 °C, c) 300 °C, and d) 400 °C.

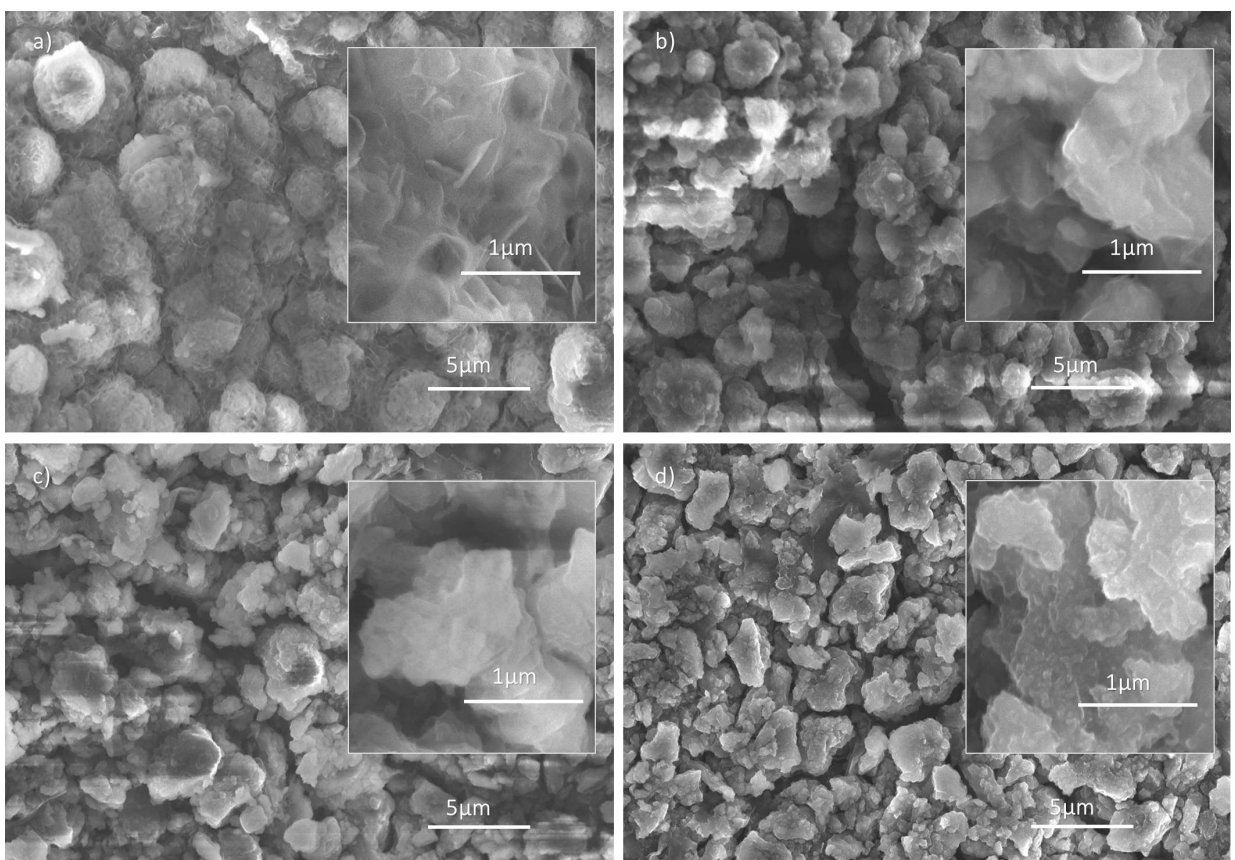


Figure 6. HRSEM images of cycled composite silicon electrodes containing P84 binder heat-treated to a) 120 °C, b) 200 °C, c) 300 °C, and d) 400 °C. The conditions of cycling: Galvanostatic cycling at C/3 rate, 50 cycles, vs. Li counter electrodes, and the electrolyte solution was 1 M LiPF₆ DMC:FEC 4:1.

Nonuniform surface films that cannot really passivate the active mass is probably the leading cause of the anodes' failure.

Uniform, passivating surface films cannot be formed due to many cracks that appear upon silicon expansion, allowing more

and more reduction of electrolyte solution's species. This leads to the formation of thicker, nonuniform, and unstable surface layers during continuous cycling experiments.

We propose that the primary factor for the enhanced performances promoted by the formation of more uniform and stable SEI types surface films that properly passivate the composite silicon electrodes containing P84 binder heat-treated to 400 °C is their significantly improved intrinsic integral characteristics. The 400 °C heat-treated P84 binder develops a relatively high tensile strength and Young's modulus, compared to this binder heated at lower temperatures, and the jnl binders that we tested. Hence, we demonstrate that the binder may play a crucial role in maintaining healthy and effective passivation of silicon anodes during their swelling upon lithiation. Increased robustness and strength of the binder lead to better maintenance and control of volume changes, prevent tearing down of the binder over cycles, and ensure the stability of the protective surface films that may naturally develop on Li, Li–C, and Li–Si anodes in the FEC containing electrolyte solution used herein (if their morphology is reasonably stable).

Sheng et al.^[36,38] studied the tensile strength and Young's modulus of P84 polyimide heated to 400 °C. The mechanical properties are enhanced in factors of 5–6 and 3–4, as compared to lower temperatures heat-treated P84 due to cross-linking process occurring in the polyimide. The adhesion strength test measured by the pull-off test showed supremacy in factors of about 1.5 and 3 of the heat-treated electrodes at 400 °C compared to 300 °C and 200 °C, respectively. As the binder's primary role in composite electrodes is to hold the silicon particles tightly and to control the volume change phenomena, the improved adhesion might significantly help.

Anjnl potential factor contributing to the improved and more stable passivating surface films on Si electrodes containing the P84 binder treated at elevated temperatures, might be reactions/interactions between the binder and the oxygenated silicon particles' surface. It has been known that the adhesion between silica and polyimides is favorable.^[43] Silicon always contains surface Si-oxide native layers, including –Si–O–Si and –Si–OH^[44,45] groups that can interact with the polymer's surface groups and solution reduction products.

Sheng et al.^[36] suggested several types of reactions that occur when P84 (Figure 7a) is exposed to high temperature heat treatment, including free radicals formation and C=N double bonds cleavage during cross-linking, releasing CO₂, hydrogen, and CONH₂, thus forming reactive intermediates like that suggested in Figure 7b. The formation of such radicals opens the door for a plethora of interactions among these moieties and between them and the native surface species on the Si particles.

We propose that at high temperatures, P84 reacts with the oxynated silicon surface groups through free radicals formed in the polymer, cleavage of the C=N double bond, and hydrogen bonds' formation.^[46,47] High temperatures enhance bond strength and promote reactions, like the formation of covalent bonds over hydrogen bonds.^[44] When more Si–O–Binder interactions are relevant, and cross-links based matrices are formed, the silicon volume changes can be better mitigated,

leading to fewer cracks in the active mass, resulting in more stable surface films that can passivate the electrodes effectively.^[43]

Figure 7c suggests schematic bonding options of the heat-treated binder on the Si surface.

Post-cycled electrodes that were prepared by heat treatment at 120 °C and 400 °C were analyzed by EDS (Figure 8). The EDS data revealed that the atomic percentage of silicon at the surface of cycled electrodes heat-treated to 400 °C was approximately 34%, whereas it is less than 3 percent at the surface of cycled electrodes that were heat-treated to 120 °C. This difference may suggest that the cycled electrodes heat-treated at the lower temperature were covered by surface layers that were too thick, so the X-rays could not pass through to detect the silicon active mass. In addition, the fluorine and oxygen content at the surface of the cycled electrodes heat-treated to 120 °C is higher compared to their content at the cycled electrodes heat-treated at 400 °C, even after normalizing the data by removing the effect of silicon. In turn, the atomic percent of carbon is higher at the surface of the cycled electrodes heat-treated at 400 °C.

Post-Mortem Analysis by X-Ray Photoelectron Spectroscopy

XPS measurements provided additional insight into the composition of the surface layers formed on the electrodes upon cycling, also conveying information about the oxidation state of the elements composing the surface films. Figure 9a provides the quantitative analysis, presenting the percentage of elements in the surface films developed on the four types of composite Si electrodes after cycling in identical experiments, differing from each jnl by the temperature of the preliminary heat treatment that the electrodes underwent. Figure 9b shows the spectra of the various elements, from which their oxidation states can be determined. Due to the shallow penetration depth of the X-rays used in XPS compared to the higher penetration depth in the EDS measurements, silicon cannot be identified in any of the samples except for traces of silicon that relate to surface interaction of the active mass with the electrolyte solution in the cells. Nonetheless, the temperature of the electrodes' preliminary heat treatment that cures the P84 binder, seems to have a pronounced effect on the surface films' composition, revealing the role of the curing process of the P84 binder on the electrodes' surface chemistry and stability. There is a trend in the results presented in Figure 9a and Figure 9b. The lithium content is the highest, and the fluorine and oxygen contents are low in the surface films formed on the cycled electrodes that were prepared by heat treatment at 400 °C. In turn, the highest relative content of fluorine and phosphorous was found in the surface films formed on the electrodes prepared at 120 °C.

The XPS data (Figure 9b), which include C, O, P, F, and Li peaks, reflect the usual surface films formed on Li-graphite and Li–Si electrodes, resulting from reducing the alkyl carbonate solvents to surface species such as Li-alkyl carbonates (e.g., CH₃OCO₂Li (CH₂OCO₂Li)₂), Li-alkoxides (e.g. CH₃OLi), Li₂CO₃ and

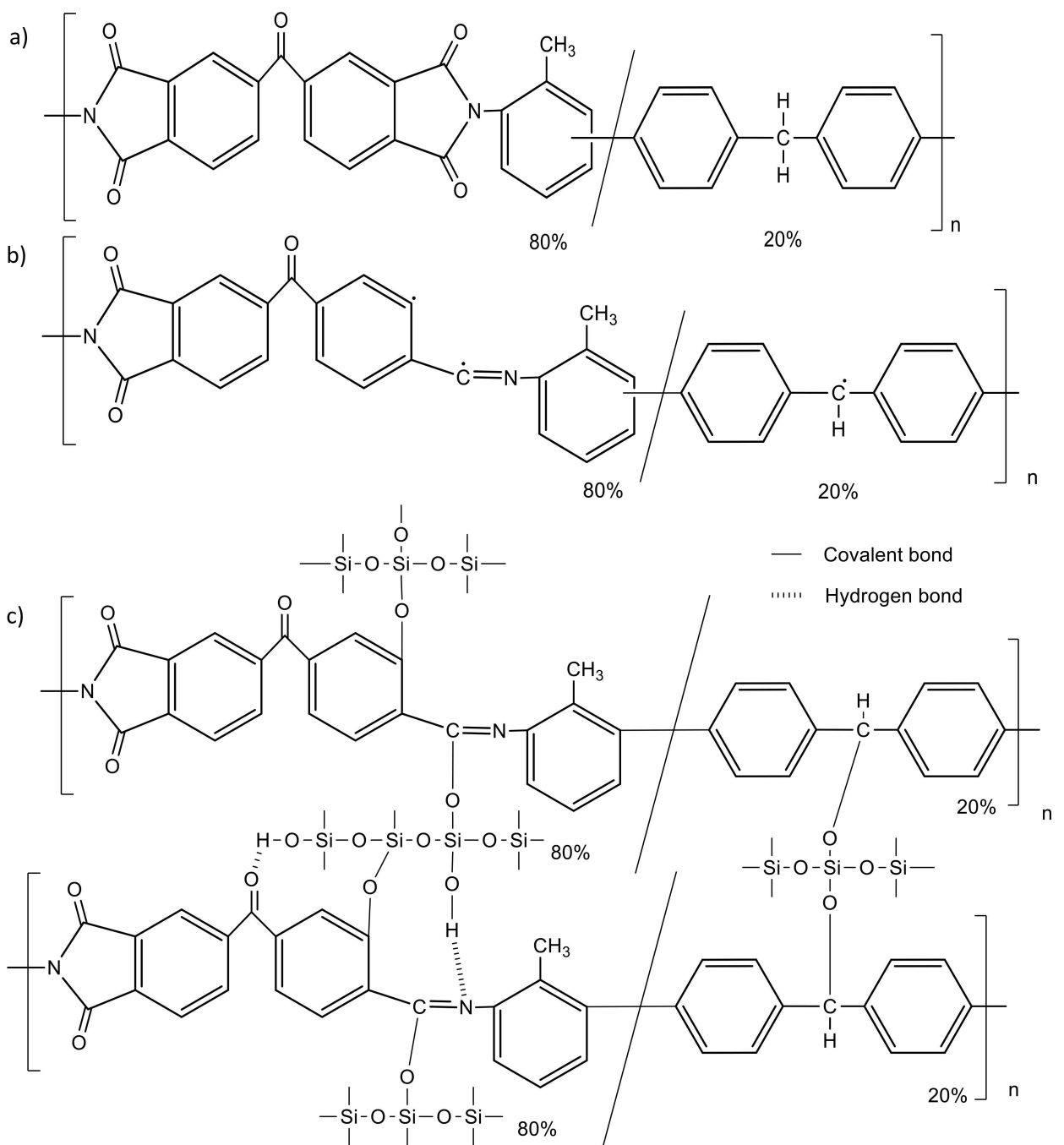


Figure 7. a) Molecular structure of P84 binder. b) One of the suggested P84 molecules after annealing^[36] and c) Options for surface interactions between heat-treated P84 molecules and the silicon active mass, which contain oxygenated surface films.

from reducing LiPF₆ to LiF, Li_xPF_y and Li_xPOF_y surface species.^[48–57]

For more details: The F1s spectrum is dominated by 685 eV and 687.5 eV peaks, characteristics of LiF, and the residual LiPF₆ decomposition species Li_xPF_y and Li_xPF_yO_z.^[48,49] The P2p 137.5 eV peak also corresponds to Li_xPF_y and Li_xPF_yO_z moieties. It fits the same trend as the F1s spectrum data, where the most comparatively intensive peaks appear in the spectra measured with cycled electrodes that were prepared at 120 °C. These peaks are the least intensive in the spectra related to the

electrodes prepared by heat treatment at 400 °C. The Li1s spectra exhibit broad and high peaks around 56 eV, corresponding to a combination of LiF, Li_xPF_y, and Li_xPF_yO_z (the latter being formed by the interaction of Li_xPF_y moieties with trace moisture).^[48] The spectra measured with the cycled electrodes prepared at 120 °C show relatively high binding energies for F, P, and Li, which can belong (most logically) to residual LiPF₆ salt. These findings and the difference in the spectra of the electrodes treated at 120 °C compared to spectra of electrodes prepared at higher temperatures can be explained by the

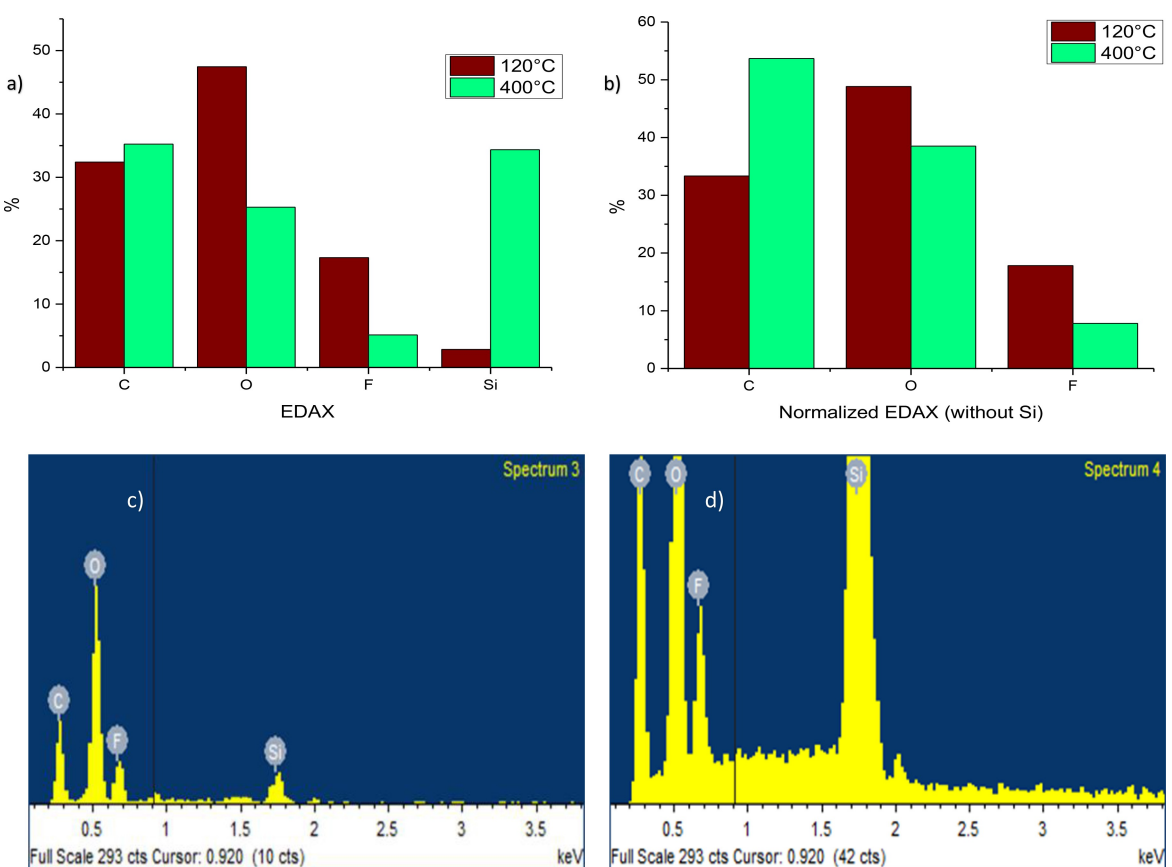


Figure 8. Elemental composition at the surface of cycled composite silicon electrodes containing P84 binder heat-treated to 120 °C and 400 °C as indicated, measured by EDS. a) comparing C, O, F, and Si atomic percentages. b) Normalized elemental composition, comparing the percentage of C, O, and F after excluding the content of Si. The conditions of cycling were Galvanostatic cycling at C/3 rate, 50 cycles, vs. Li counter electrodes, and the electrolyte solution was 1 M LiPF₆ DMC:FEC 4:1. EDS mapping of the cycled composite silicon electrodes containing P84 binder heat-treated to c) 120 °C and d) 400 °C.

different composite structures of the various types of electrodes: since at 120 °C the P84 binder does not undergo significant changes, the composite electrodes are affected strongly by the periodic volume changes, they become cracked and porous, thereby, it is very hard to get rid of residual trapped LiPF₆ salt traces therein. When the electrodes are treated at high enough temperatures, the P84 undergoes thermal interactions that strengthen the composite structure, making it more robust, enabling the development of stable, passivating surface films that, because of their high quality, are thin, thanks to the strong passivation that they provide.

The most striking result presented in Figure 9b is the relatively low binding energies of all the elements in the spectra measured from the electrodes prepared at 400 °C. Low binding energies reflect reduced species. Lithiation of silicon produces highly reactive reducing agents with the general stoichiometry Li_xSi (0 < x < 4.2). Hence, all the surface species on these anodes are formed in reduction processes by highly reactive reducing agents. At the end of discharge, the composite silicon electrodes should contain some residual Li. Hence, they remain with reduced capability. Thereby, the photoelectron spectra of such electrodes are expected to represent elements at low oxidation states, which means elements' XPS peaks appear at low binding energy values, provided that the electrodes are passivated

properly. This is exactly what the charts of Figure 9b reflect. We describe below some interesting spectral features.

Li₂O peaks are very prominent in the spectra of the electrodes prepared at 400 °C. They are reflected by Li1s and O1s peaks at 54 eV and 528.5 eV, respectively. Lithium oxide is the natural final product of SiO, SiO₂ lithiation. Signals of phosphates (Li_xPO_yF_z type moieties at all kinds of possible stoichiometries) and Li₂CO₃, which are often present in the SEI layer formed on Li, lithiated carbons, and silicon species when alkyl carbonates / LiPF₆ solutions are used, were also found in all the photoelectron spectra of the cycled electrodes. Interestingly, simple phosphates (PO_x compounds) were hardly detected by the spectra obtained from cycled electrodes prepared at 120 °C.

The C1s spectra of the electrodes prepared at 400 °C show a pronounced peak at 283 eV that can be assigned to either lithiated carbon Li_xC or silicon carbide Si—C.^[50–54] The carbon peaks around 285 eV belong to alkane and alkene fractions.^[50,55] The peaks around 286.5 eV relate to C—O bonds (e.g., CH₃—O—Li), and the peaks around 289.5 eV relate to carbonate groups O₂—C=O, like Li₂CO₃ or CH₃OCO₂Li.^[50,56,57] For the O1s spectral features, the peaks around 530.8 eV, correspond to lithium alkoxides R—O—Li (or Li_xSiO_y), and peaks around 532.3 eV may relate to CO_x or SiO₂.^[50,52,57] These XPS data reflect so well

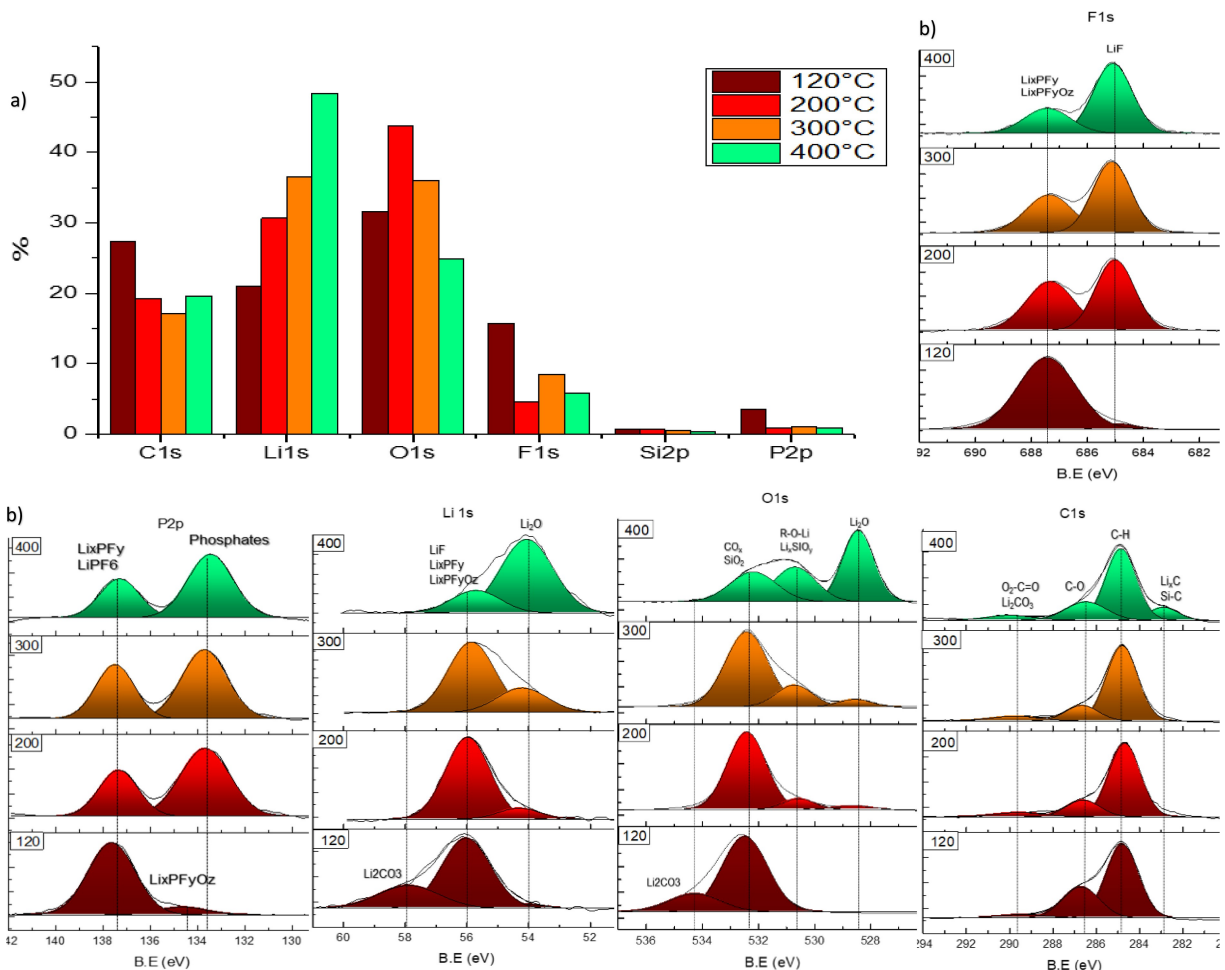


Figure 9. a) Elemental (atomic) composition of the surface films formed on cycled composite silicon electrodes containing P84 binder heat-treated to 120 °C, 200 °C, 300 °C and 400 °C determined by XPS. The conditions of cycling were Galvanostatic cycling at C/3 rate, 50 cycles, vs. Li counter electrodes, and the electrolyte solution was 1 M LiPF₆ DMC:FEC 4:1. b) F1s (a), P2p (b), Li1s (c), O1s (d), and C1s (e) peaks obtained by XPS measurements of cycled composite silicon electrodes containing P84 binder heat-treated to 120 °C, 200 °C, 300 °C and 400 °C as indicated. The spectra reflect the composition of the surface films formed on the electrodes upon galvanostatic cycling (50 cycles) at C/3 rate vs. Li counter electrodes with electrolyte solutions of 1 M LiPF₆ DMC:FEC 4:1.

the general surface chemistry developed on all kinds of negative electrodes in conventional alkyl-carbonates/LiPF₆ solutions.

In conclusion, the XPS results of the cycled electrodes prepared at 400 °C, which show indeed low binding energy spectra of surface species, mean that these electrodes are passivated very effectively, demonstrating a very strong effect of the binder's properties on the composite Si anodes surface chemistry and their performance. The results of all the measurements we have carried out in this work converge in the conclusion section below.

Conclusions

Our studies demonstrate a significant influence of the binder properties on the behavior and characteristics of composite Si anodes in Li-ion battery prototypes. The binder's mechanical strength and integrity may reduce pronouncedly the negative effect of the periodic volume change of Si anodes upon cycling.

By controlling these volume fluctuations, it is possible to promote the formation of stable, passivating SEI type surface films despite the intrinsic morphological instability of lithiating/de-lithiating Si anodes in Li-ion cells. In this work, we demonstrated a very interesting methodology of tuning binders' properties through thermal pre-treatments as a single mean. P84 as a binder enabled these properties to be tuned by simple heat treatments. It was discovered that composite Si electrodes containing P84 binder could reach improved capabilities thanks to heat treatment at 400 °C. For this study, we used in purpose a very simple and relatively cheap Si material comprising micrometric size particles. The heat-treated electrodes were tested in half (vs. Li CE) and full (vs. Ni-rich NCM622 cathodes) cells. Post-mortem analysis was carried out using a mechanical robustness test, and imaging was done using HR scanning electron microscopy, EDS, and XPS. All the results we obtained converged very nicely.

It appears that the heat treatment at high enough temperatures enhances the adherence of the composite active mass to the copper foils current collectors, reduces electrodes delamina-

tion, and positively controls the growth of passivating SEI type surface layers. The microscopic studies showed that the heat treatment at high enough temperatures forms a rigid and strong binder that can mitigate the negative effect of the periodic volume changes of these electrodes upon cycling, enabling the development of effective passivation by surface films formed via the usual surface chemistry of Li, Li–C, Li–Si electrodes in conventional electrolyte solutions.

The composite Si anodes containing the appropriately cured P84 binder outperformed composite silicon anodes based on advanced binders like LiPAA and Na-alginate. The electrodes presented herein are far from being optimal and suitable for any commercial applications. However, the studies demonstrate positive trends and positive directions that can help in further optimization efforts of high specific capacity Si anodes for high energy density Li-ion cells.

Conflict of Interests

The authors declare no conflict of interest.

Data Availability Statement

The data that support the findings of this study are available from the corresponding author upon reasonable request.

Keywords: Li ion batteries • Si anodes • polymeric binders • NCM622 cathodes

- [1] P. Li, H. Kim, S. T. Myung, Y. K. Sun, *Energy Storage Mater.* **2021**, *5*, 550–576 Preprint at <https://doi.org/10.1016/j.ensm.2020.11.028>.
- [2] L. Sun, et al., *Energy Storage Materials* **2022**, *46*, 482–502 Preprint at <https://doi.org/10.1016/j.ensm.2022.01.042>.
- [3] X. Zuo, J. Zhu, P. Müller-Buschbaum, Y. J. Cheng, *Nano Energy* **2017**, *31*, 113–143 Preprint at <https://doi.org/10.1016/j.nanoen.2016.11.013>.
- [4] W. F. Ren, Y. Zhou, J. T. Li, L. Huang, S. G. Sun, *Curr. Opin. Electrochem.* **2019**, *18*, 46–54 Preprint at <https://doi.org/10.1016/j.coelec.2019.09.006>.
- [5] D. Ma, Z. Cao, A. Hu, *Nano-Micro Lett.* **2014**, *6*, 347–358.
- [6] M. N. Obrovac, L. Christensen, D. B. Le, J. R. Dahn, *J. Electrochem. Soc.* **2007**, *154*, A849.
- [7] M. Ashuri, Q. He, L. L. Shaw, *Nanoscale* **2016**, *8*, 74–103.
- [8] S. Okashy, S. Luski, Y. Elias, D. Aurbach, *J. Solid State Electrochem.* **2018**, *22*, 3289–3301.
- [9] M. N. Obrovac, V. L. Chevrier, *Chem. Rev.* **2014**, *114*, 11444–11502.
- [10] Y. Cui, *Nat. Energy* **2021**, *6*, 995–996 Preprint at <https://doi.org/10.1038/s41560-021-00918-2>.
- [11] D. Schneider, *IEEE Spectrum* **2019**, *56* (1), 48–49.
- [12] K. Turcheniuk, et al., *Nature* **2018**, *559*, 467–470.
- [13] H. Li, et al., *Advanced Energy Materials* **2022**, *12*, 2102181, Preprint at <https://doi.org/10.1002/aenm.202102181>.
- [14] <https://www.enovix.com/>.
- [15] <https://amprius.com/>.
- [16] <https://www.silanano.com/>.
- [17] <https://group14.technology/en/>.
- [18] J. W. Choi, D. Aurbach, *Nat. Rev. Mater.* **2016**, *1*, 16013.
- [19] T. W. Kwon, J. W. Choi, A. Coskun, *Chem. Soc. Rev.* **2018**, *47*, 2145–2164.
- [20] D. Linden, *Linden's Handbook of Batteries*. Reddy, Thomas **2010**. doi: 10.1016/0378-7753&DELETE;TRzwj;(86)80059-3.
- [21] J. T. Li, et al., *Adv Energy Mater* **2017**, *7*, 1–30.
- [22] G. Liang, J. Zhu, A. Chen, Q. Yang, C. Zhi, *npj Flexible Electronics* **2021**, *5*, 27, Preprint at <https://doi.org/10.1038/s41528-021-00124-w>.
- [23] J. Choi, et al., *ACS Appl Mater Interfaces* **2015**, *7*, 14851–14858.
- [24] Y. M. Lee, et al., *J Power Sources* **2014**, *252*, 138–143.
- [25] D. Bresser, D. Buchholz, A. Moretti, A. Varzi, S. Passerini, *Energy Environ. Sci.* **2018**, *11*, 3096–3127.
- [26] Y. H. Kim, G. F. Walker, J. Kim, J. Park, *J. Adhes. Sci. Technol.* **1987**, *1*, 331–339.
- [27] J. S. Kim, et al., *J Power Sources* **2013**, *244*, 521–526.
- [28] K. W. Lee, G. F. Walker, A. Viehbeck, *J. Adhes. Sci. Technol.* **1995**, *9*, 1125–1141.
- [29] K.-M. Chen, et al., *J Appl Polym Sci* **1992**, *45*, 947–956.
- [30] W. Jang, M. Seo, J. Seo, S. Park, H. Han, *Polym. Int.* **2008**, *57*, 350–358.
- [31] H. Kim, J. Jang, *Corrosion Protection – Adhesion Promotion for Polyimide/Copper System Using Silane-Modified Polymeric Materials*.
- [32] H. Ishida, K. Kelley, *J. Adhes.* **1991**, *36*, 177–191.
- [33] <https://www.p84.com/en/>.
- [34] Q. Zhang, X. Li, J. Dong, X. Zhao, *Engineering Polymer Research* **2022**, *5*, 107–116 Preprint at <https://doi.org/10.1016/j.aiepr.2022.03.004>.
- [35] J. Oh, et al., *ACS Omega* **2017**, *2*, 8438–8444.
- [36] L. Sheng, et al., *J. Memb. Sci.* **2020**, *595*, 117580.
- [37] M. B. Saeed, M. S. Zhan, *Eur. Polym. J.* **2006**, *42*, 1844–1854.
- [38] L. Sheng, et al., *Sep Purif Technol* **2021**, *256*, 117741.
- [39] E. P. Favvas, et al., *Journal of Porous Materials* **2008**, *15*, 625–633.
- [40] M. J. Loveridge, et al., *Sci Rep* **2016**, *6*, 37787.
- [41] M. N. Obrovac, L. J. Krause, *J. Electrochem. Soc.* **2007**, *154*, A103.
- [42] Y. He, et al., *J Power Sources* **2012**, *216*, 131–138.
- [43] C. Den Besten, *Proceedings IEEE Micro Electro Mechanical Systems* **1992**, 104–109.
- [44] N. S. Hochgatterer, et al., *Electrochemical – Solid-State Letters* **2008**, *11* (5), A76–A80.
- [45] Y. M. Lee, J. Y. Lee, H.-T. Shim, J. K. Lee, J.-K. Park, *J. Electrochem. Soc.* **2007**, *154*, A515.
- [46] Z. Lu, et al., *Eur Polym J* **2018**, *102*, 209–218.
- [47] M. Hashizume, S. Fukagawa, S. Mishima, T. Osuga, K. Iijima, *Langmuir* **2016**, *32*, 12344–12351.
- [48] B. S. Parimalam, B. L. Lucht, *J. Electrochem. Soc.* **2018**, *165*, A251–A255.
- [49] C. Cao, et al., *Joule* **2019**, *3*, 762–781.
- [50] T. Jaumann, et al., *Physical Chemistry Chemical Physics* **2015**, *17*, 24956–24967.
- [51] S. Link, et al., *Electrochim Acta* **2021**, *380*, 138216.
- [52] K. Ciosek Höglström, et al., *Journal of Physical Chemistry C* **2013**, *117*, 23476–23486.
- [53] M. Ahmed, et al., *Nanotechnology* **2015**, *26*, 434005.
- [54] X. Dou, et al., *Small Methods* **2019**, *3* (4), 1800177.
- [55] S. Dalavi, P. Guduru, B. L. Lucht, *J. Electrochem. Soc.* **2012**, *159*, A642–A646.
- [56] G. Salitra, et al., *ACS Appl Mater Interfaces* **2018**, *10*, 19773–19782.
- [57] V. Etacheri, et al., *Langmuir* **2012**, *28*, 965–976.

Manuscript received: April 12, 2024
Revised manuscript received: June 13, 2024
Accepted manuscript online: June 16, 2024
Version of record online: July 29, 2024